Published in final edited form as:
Mech Dev. 2012 September ; 129(9-12): 193–207. doi:10.1016/j.mod.2012.08.002.

Early embryonic lethality of mice with disrupted transcription cofactor PIMT/NCOA6IP/Tgs1 gene

Yuzhi Jia, **Navin Viswakarma**, **Susan E. Crawford**[1], **Joy Sarkar**, **M. Sambasiva Rao**, **William Karpus**, **Yashpal S. Kanwar**, **Yi-Jun Zhu**[*], and **Janardan K. Reddy**[*]

Department of Pathology, Feinberg School of Medicine, Northwestern University, Chicago, IL 60611-3008, USA

Abstract

PIMT (also known as PIPMT/NCOA6IP/Tgs1), first isolated as a transcription coactivator PRIP (NCOA6)-interacting 96-kDa protein with RNA-binding property, possesses RNA methyltransferase activity. As a transcription coactivator binding protein, PIMT enhances the nuclear receptor transcriptional activity and its methyltransferase property is involved in the formation of the 2,2,7-trimethylguanosine cap of non-coding small RNAs, but the in vivo functions of this gene have not been fully explored. To elucidate the biological functions, we used gene targeting to generate mice with a disrupted PIMT/Tgs1 gene. Disruption of PIMT gene results in early embryonic lethality due to impairment of development around the blastocyst and uterine implantation stages. We show that PIMT is expressed in all cells of the E3.5 day blastocyst in the mouse. PIMT null mutation abolished PIMT expression in all cells of the blastocyst and caused a reduction in the expression of Oct4 and Nanog transcription factor proteins in the E3.5 blastocyst resulting in the near failure to form inner cell mass (ICM). With conditional deletion of PIMT gene, mouse embryonic fibroblasts (MEFs) exhibit defective wound healing in the scratch assay and a reduction in cell proliferation due to decreased G_0/G_1 transition and G_2/M phase cell cycle arrest. We conclude that PIMT/NCOA6IP, which is expressed in all cells of the 3.5 day stage blastocyst, is indispensable for early embryonic development.

Keywords

PIMT/ NCOA6IP/Tgs1; Embryonic lethality; Apoptosis; Blastocyst; G_2/M phase arrest; Mouse Embryonic Fibroblasts; Defective wound healing

1. Introduction

The mechanisms underlying the transcriptional activation by nuclear receptors are complex, in part, due to the participation in this process of many transcription coactivators (Conaway et al., 2005; Fondell et al., 1996; Hermanson et al., 2002; Kornberg, 2007; Lonard and O'Malley, 2006; Roeder, 2005; Spiegelman and Heinrich, 2004). Although coactivators play an important role in enhancing gene expression mediated by liganded nuclear receptors, the

[*]Corresponding authors: Tel.: +1 312 503 7948; Fax: +1 312 503 8249. y-zhu@northwestern.edu (Y. Zhu) or jkreddy@northwestern.edu (J.K. Reddy). .
[1]Current address: St. Louis University, Dept of Pathology, 1402 S. Grand Blvd, St. Louis MO 63104

significance of the existence of ~300 coactivators and their functions remain largely unclear (Lonard and O'Malley, 2006; Reddy et al., 2006; Yu and Reddy, 2007). Some of these coactivators form multisubunit protein complexes, but the events controlling their assembly and disassembly, and their involvement in gene and cell specific transcription are poorly understood (Conaway et al., 2005; Hermanson et al., 2002; Kornberg, 2007; Lonard and O'Malley, 2006; Roeder, 2005; Shang et al., 2000). As transcription enhancers, coactivators fall into different functional categories (Roeder, 2005; Viswakarma et al., 2011; Yu and Reddy, 2007). Some function as chromatin-remodeling complexes, while others serve as histone-modifying complexes (Hermanson et al., 2002; Kornberg, 2007; Lewis and Reinberg, 2003; Roeder, 2005). Furthermore, other coactivators, with no known enzymatic activity, provide linkage of activated receptor to the components of core TFIID basal transcription apparatus (Auboeuf et al., 2005; Conaway et al., 2005; Fondell et al., 1996; Kornberg, 2007; Lewis and Reinberg, 2003; Roeder, 2005). Accordingly, these classes of coactivator complexes participate in the unwinding of chromatin, covalent modification of histones, and the facilitation of access of transcriptional machinery to the promoter region of target genes (Auboeuf et al., 2005; Conaway et al., 2005; Kornberg, 2007; Lemon et al., 2001; Roeder, 2005). While detailed knowledge of specific functions of a majority of coactivators is lacking, there is an increasing recognition of the general importance of a selected set of these molecules in gene expression, embryogenesis, cell growth and differentiation (Conaway et al., 2005; Fondell et al., 1996; Hermanson et al., 2002; Roeder, 2005; Reddy et al., 2006; Spiegelman and Heinrich, 2004; Viswakarma et al., 2011).

This burgeoning field of nuclear receptor coactivators started with the cloning, in 1995, of SRC-1, the first member of a 3 member p160 family of coactivators, with histone acetyltransferase activity (Hermanson et al., 2002; Lonard and O'Malley, 2006; Onate et al., 1995; Reddy et al., 2006). TIF-2/GRIP-1 (SRC-2), and ACTR/AIB/pCIP (SRC-3) are the other two members of this p160 family (Lonard and O'Malley, 2006; Viswakarma et al., 2010; Wang et al., 2006; Xu et al., 2000; Yu and Reddy, 2007). Further search for coactivators, by many laboratories over the years, has led to the identification of a plethora of proteins (Lonard and O'Malley, 2006; Mahajan and Samuels, 2008; Surapureddi et al., 2002; Viswakarma et al., 2011; Yu and Reddy, 2007). We and others have been focusing on two of these molecules, namely PBP/TRAP220/DRIP205/ MED1 (Ito et al., 2000; Rachez et al., 1999; Yuan et al., 1998; Zhu et al., 1997; 2000a), and PRIP/ASC-2/ NRC/TRBP/ RAP250/ NCOA6 (Mahajan and Samuels, 2008; Viswakarma et al., 2010; Zhu et al., 2000b). PBP, first cloned in our laboratory, in 1997, as peroxisome proliferator-activated receptor (PPAR)-binding protein (Zhu et al., 1997), was subsequently identified as a component MED1 of the Mediator complex comprised of at least 25 subunit proteins (Conaway et al., 2005; Fondell et al., 1996; Kornberg, 2007; Rachez et al., 1999). Mediator complex functions as a molecular bridge between enhancer-bound receptors and the components of the basal transcription apparatus (Conaway et al., 2005; Kornberg, 2007). Disruption of MED1 gene results in mediator complex disassembly and leads to mid-gestational embryonic lethality in the mouse (Crawford et al., 2002; Ito et al., 2000; Zhu et al., 2000a). Of interest is that conditional deletion of this gene in liver abrogates nuclear receptor PPARα and CAR functions (Jia et al., 2004, 2005; Matsumoto et al., 2007). Likewise, disruption of NCOA6 gene also causes embryonic lethality but the conditional deletion of this gene in liver does not affect PPARα and constitutive androstane receptor (CAR) functions (Mahajan and Samuels, 2008; Viswakarma et al., 2010). Since germ-line knockout of MED1 or NCOA6 leads to embryonic lethality, it raises the issue of the role of other coactivators in embryonic development and cell specific functions (Mahajan and Samuels, 2008; Reddy et al., 2006; Yu and Reddy, 2007; Viswakarma et al., 2010).

Our laboratory first identified PIMT (PIPMT/NCOA6IP) as PRIP/NCOA6-interacting protein (Zhu et al., 2001). Subsequently, a number of laboratories identified other proteins

that interact with NCOA6 and some of these proteins have been shown to form a multi-subunit, ~2Mda protein complex designated ASCOM (Mahajan and Samuels, 2008). Although NCOA6 has also been found to be a component of two other protein complexes, namely ALR/MLL2 and PTIP (Auboeuf et al., 2005; Cho et al., 2007; Mahajan and Samuels, 2008), PIMT is not known to be associated with any known coactivator complexes (Yu and Reddy, 2007). Nevertheless, it is possible that PIMT may form a complex comprising of NCOA6, CBP/p300, and MED1, as these molecules have been shown to interact with PIMT (Misra et al., 2002). PIMT binds *S*-adenosyl-L-methionine, the methyl donor for methyltransferase reaction (Enunlu et al., 2003; Girard et al., 2008; Zhu et al., 2001). It also binds RNA, suggesting that it functions as an RNA methyltransferase, in addition to its coactivator function (Zhu et al., 2001). Consistent with these observations, PIMT homologue in the yeast has been shown to be essential for hypermethylation of the m^7G caps of both snRNAs and snoRNAs (Girard et al., 2008; Mouaikel et al., 2002). This RNA hypermethylase activity of PIMT is responsible for m_3G cap formation of U small nuclear RNAs (U snRNAs) and small nucleolar RNAs (snoRNAs) and is also needed for the capping of unspliced and partially spliced HIV-1 RNAs (Girard et al., 2008; Mouaikel et al., 2002; Yadavalli and Jeang, 2010). In addition, PIMT/Tgs1 also hypermethylates RNA subunit of telomerase (TER1) and thus maintains chromosomal integrity (Tang et al., 2012). Furthermore, the *Drosophila* homologue of PIMT has been shown to play an essential role in development (Komonyi et al., 2005). In view of the dual functions of PIMT gene, namely involvement in transcription and RNA hypermethylation (Misra et al., 2002; Zhu et al., 2001), it appeared necessary to explore the expression pattern of PIMT and certain key coactivators in vivo during embryonic development. In order to better understand the biological function of PIMT in mammalian pathophysiology, we used gene targeting to inactivate the *PIMT/NCOA6IP* gene in mice. PIMT heterozygous mice display no obvious phenotype and males and females are fertile. We obtained no nullizygous mice from $PIMT^{+/-}$ intercrosses, indicating that the disruption of PIMT is embryonic lethal in mice. Furthermore, PIMT-null embryos were not observed at postimplantation stages. $PIMT^{-/-}$ blastocysts were recovered which revealed increased apoptosis, reduced cell density and impairment of inner cell mass (ICM) development. We conclude that PIMT is essential for the early development of mouse embryos in view of its role in gene transcription and RNA methylation.

2. Results and Discussion

2.1. PIMT gene evolution

PIMT, a RNA-binding protein with RNA methyltransferase activity, was identified originally as a transcription coactivator PRIP (NCOA6)-interacting protein (Zhu et al., 2001). The full-length PIMT cDNA of human (NP_079107) and mouse (N_P473430) encodes a protein of 853 amino acids with an estimated molecular mass of ~96.5 kDa (Zhu et al., 2001). As a coactivator-binding protein, PIMT enhances the transcriptional activity of nuclear receptors. We have previously shown that PIMT homologous proteins exist in *Saccharomyces Cerevisiae* (YPL157WP), *Arabidopsis thaliana*, and *Caenorhabditis elegans* (Zhu et al., 2001). The yeast homolog of PIMT has been shown to exhibit trimethylguanosine synthase (Tgs1) activity, the RNA methyltransferase responsible for the hypermethylation of the 5′ m^7G cap structure of snRNAs and snoRNAs (Girard et al., 2008; Mouaikel et al., 2002). Accordingly, PIMT/Tgs1 as originally proposed, exhibits dual critical cellular functions in that it serves as a transcription cofactor and as an RNA hypermethylating enzyme (Enunlu et al., 2003; Mouaikel et al., 2002; Yadavalli and Jeang, 2010; Yu and Reddy, 2007; Zhu et al., 2001). Analysis of currently available eukaryotic genome assemblies and expressed sequence tags (ESTs) strongly suggests the existence of a single PIMT/Tgs1 homolog in 16 representative species when human PIMT is used as an

out-group in the phylogenetic tree construction (http://www.treefam.org/cgi-bin/TFseq.pl?id=ENSG00000137574). Conservation of RNA methyltransferase domain in the C-terminal region of PIMT proteins at the amino acid level in ten different eukaryotic species, suggests that PIMT gene arose early in eukaryotic evolution.

2.2. PIMT expression during mouse embryonic development

Expression of PIMT in different cell types during development was first examined by immunohistochemical staining of E16.5 mouse embryos. As illustrated in Fig. 1, PIMT expression is predominantly nuclear in location but some diffuse staining in the cytoplasm was also observed. In humans, PIMT/Tgs1 long isoform locates in the cytoplasm and a short isoform in mostly nuclear in location (Verheggen and Betrand, 2012). We now show that PIMT staining in the mouse embryo is prominent in the brain tissue surrounding the ventricle (Fig. 1A, B), growing enamel bud (Fig. 1C, D), lung (Fig. 1E), liver (Fig. 1F), intestinal mucosal crypt cells (Fig. 1G) and the germinal epithelium of testis (Fig. 1H). In the E16.5 embryonic liver, PIMT expression was prominent in both hepatocytes and hematopoietic cells (Fig. 1F). PIMT staining was also noted in the heart, pancreas, kidney, testis and basal cells of the skin epidermis (data not shown). Western blotting revealed PIMT as a ~ 100 kDa protein during E10.5 to E18.5 days of embryonic development (Fig. 1I). EST data base analysis revealed that PIMT is expressed in all developmental stages in the mouse embryo. We performed quantitative PCR analysis of PIMT and selected key transcription cofactors such as CBP, MED1 and PRIP in the developing E10.5 to E18.5 mouse embryos (Fig. 2). Both PRIP and PIMT expressed at high levels during E10.5 and E16.5 but decreased at E18.5 (Fig. 2). The expression of MED1 and CBP, which also interact with PIMT (Misra et al., 2002), paralleled PIMT and PRIP expression. Of the nuclear receptors examined by quantitative PCR, PPARα displayed a distinct late expression pattern (E14.5 to E16.5 days) as compared to the expression of PPARβ/δ and PPARγ, the other two members of PPAR subfamily (Fig. 2). The expression of RXR, the heterodimerization partner of some nuclear receptors, appeared similar to that noted for PPARβ/δ and PPARγ, except that RXR expression was decreased at E18.5 (Fig. 2).

2.3. Disruption of PIMT gene in mice

To elucidate the function of PIMT in mammals, we constructed a conditional knock-out allele using the two-*loxP*, two-*frt* recombination system, according to the strategy depicted in Fig. 3A. This gene-targeting vector was designed to delete exons 3 and 4 (Fig. 3A). These two exons code for amino acids 57-381 and removal of this segment of PIMT would likely interfere with the interaction of PRIP with PIMT (Zhu et al., 2001). It should be noted that cDNA fragment directly recovered by yeast-two hybrid screening, with PRIP as bait, encodes N-terminal amino acids 1-384 of PIMT, suggesting that PIMT N-terminal region is important for its interaction with coactivator PRIP (Zhu et al., 2001). In this study, we used GST-pull-down assays to confirm the binding of [^{35}S]-labeled N-terminal domain of PIMT (1-369 amino acids) with GST-PRIP (Fig. 3B; upper panel). Binding of this N-terminal PIMT to the PIMT-binding domain of PRIP (PRIP 773-927 amino acids) was observed (Fig. 3B). Furthermore, we found no appreciable binding of [^{35}S]-labeled PRIP (PIMT-binding domain) to GST-PIMT-C-terminal domain (577-852 amino acids) but the binding to PIMT-N fragment was robust (Fig. 3B; lower panel). Thus, we conclude that PRIP-binds with the N-terminal but not with the C-terminal domain of PIMT protein. We, therefore, reasoned that deletion of the N-terminal PIMT would interfere with its binding to PRIP and impact on PIMT function. Accordingly, the gene targeting constructs were designed to address the consequence of inhibiting this interaction in vivo. Because exons 2 and 5 are in-frame in the targeting construct, truncated protein could theoretically be produced but such a truncated protein, in general, is rapidly degraded. It is known that mis-folded truncated proteins are rapidly degraded by proteosome complexes even at the 2-cell stage embryos and later in

mouse development (Evsikov et al., 2004; Hamatani et al., 2004). As shown in section 2.8, PIMT is not detected in PIMT$^{-/-}$ MEFs.

The targeting construct was transfected by electroporation into HM1 ES cells. After selection with G418 and ganciclovir, 4 of the original 248 colonies obtained were shown to be targeted correctly for the *PIMT/PIPMT* locus by Southern blot hybridization (Fig. 3C). These four clones were karyotyped to ensure genomic integrity, and three of these targeted ES clones were then injected into C57BL/6J mouse blastocysts and transplanted into pseudopregnant C57BL/6J females. Chimeric mice obtained from these three ES clones were bred with wild-type C57BL/6J female and germline transmission was achieved. Subsequently, PIMTfl/fl-frt-neo-frt mice were crossed with FLP1 recombinase variant transgenic deleter mice to achieve *neo* deletion. These *Neo* deleted PIMT$^{flox/flox}$ mice were then crossed with EIIa-Cre transgenic mice to generate mice with germline PIMT deletion.

2.4. Disruption of PIMT gene results in early embryonic lethality

The heterozygous mice exhibit normal stature, are fertile, and do not display any obvious overt phenotypic abnormalities. We intercrossed heterozygous PIMT$^{+/-}$ mice to ascertain the viability of PIMT-null homozygotes (PIMT$^{-/-}$). The genotypes of the offspring were determined by Southern blotting and PCR analysis of tail DNA at weaning (Fig. 3D,E). Among a total of 206 weanlings genotyped, 71 were wild-type (*PIMT*$^{+/+}$), and 135 were heterozygous (*PIMT*$^{+/-}$) for the targeted allele (Table 1). The complete absence of homozygous mutants (*PIMT*$^{-/-}$) and the expected 1:2 Mendelian wild-type-to-heterozygous ratio indicated that PIMT deficiency leads to embryonic death.

To determine the stage of embryogenesis at which the PIMT gene disruption is lethal, we dissected embryos from the heterozygous intercrosses at different stages of embryonic development and genotyped. No PIMT null embryos were found at E9.5, E8.5 or E7.5 of embryonic development (Table 1). Serial sectioning of E5.5 deciduas revealed smaller, growth arrested PIMT$^{-/-}$ embryos with pyknotic nuclei and apoptotic changes as compared to PIMT$^{+/+}$ embryos (Fig. 4A,B). These observations suggest that PIMT$^{-/-}$ embryos begin to degenerate possibly commencing at the blastocyst stage and die around E5.5 without progressing further to egg cylinder stage (Fig. 4A,B). Examination of serial sections from E6.5 (Fig. 4C,D) and E7.5 (Fig. 4E,F) deciduas did not reveal any evident embryonic material in approximate location where embryo should be present. If presumptive PIMT null embryos progressed to E6.5 days they had to be completely resorbed (Fig. 4D,F). In view of these findings, we conclude that PIMT$^{-/-}$ embryos might die at the blastocyst / preimplantation stage.

2.5 Characterization of PIMT-null E3.5 day blastocysts

To analyze the embryonic lethality associated with the PIMT-null mutation in mice, we isolated E3.5 day blastocysts from heterozygous intercrosses. On PCR genotyping, 15 PIMT$^{-/-}$, 40 PIMT$^{+/-}$, and 20 PIMT$^{+/+}$ blastocysts were detected among a total of 75 in expected Mendelian ratios (Table. 1; Fig. 5A). RT-PCR analysis of E3.5 blastocysts with the primers designed flanking exons 3 and 4 revealed the expression of PIMT in PIMT$^{+/+}$ but not in PIMT$^{-/-}$ embryos (Fig. 5B). We first examined PIMT protein expression in wild-type E3.5 blastocysts using whole-mount fluorescent immunostaining and laser confocal microscopy and found nuclear expression of this protein in all cells within the blastocyst, including trophectoderm and ICM (Fig. 5C). In contrast, Oct4 and Nanog transcription factor proteins were detected only in the cells of ICM at this stage (Fig. 5C). Oct-4 and Nanog are required for specifying the differentiation of the pluripotent cells of ICM in mouse blastocysts (Nichols et al., 1998; Chambers et al., 2003; Mitsui et al., 2003; Chazaud

et al., 2006; Rossant and Tam, 2009; Gasperowicz and Natale, 2011). Cdx2 is strongly expressed in trophectoderm, which also expressed PIMT (not illustrated).

As expected, PIMT protein was not detected in any cell in PIMT$^{-/-}$ E3.5 blastocyst (Fig. 5C). Surprisingly, in PIMT$^{-/-}$ blastocysts, the expression of both Oct4 and Nanog proteins was markedly diminished or absent suggesting that PIMT deficiency results in a reduction or loss in ICM (Fig. 5C). Several mechanisms are responsible for the loss of ICM in PIMT null blastocysts: (i) differentiation of ICM is impaired, (ii) ICM cells undergo apoptosis, (iii) ICM cells fail to proliferate, expand and differentiate and (iv) cell proliferation is generally reduced while cell death is increased. DAPI staining revealed evidence of nuclear fragmentation suggestive of apoptotic changes in freshly isolated PIMT deficient blastocyst cells (Fig. 5C). Further detailed studies are needed to investigate the expression of other molecules such as Sox2, Eomes, Gata3 and Tead4 in PIMT deficient E3.5 blastocysts and the possible early onset of PIMT mutant phenotype. As pointed out above, PIMT mRNA is expressed as early as in the two-cell embryo stage (E0.5 – 1.0) and thus may be crucial in early embryogenesis (Evsikov et al., 2004; Hamatani et al., 2004). It is possible that the first few cell divisions in PIMT-deficient embryos are completed due to the presence of maternally derived PIMT mRNA in the oocytes (Eviskov et al., 2004).

2.6. Changes in other transcription cofactors in PIMT deficient blastocysts

Because PIMT is a transcription cofactor and expressed at early developmental stages, we considered it necessary to analyze the expression of other transcription cofactors in E3.5 PIMT$^{+/+}$ embryos by RT-PCR. We found a robust expression of PRIP and SRC-1 in E3.5 PIMT$^{+/+}$ embryos (Fig. 6A). CBP expression was low when compared to PIMT, PRIP, MED1 and SRC-1. Of the three members of PPAR subfamily, PPARγ and PPARδ/β expression appeared robust in E3.5 embryo as compared to very low level of PPARα expression (Fig. 6A). Quantitative PCR data showed that in PIMT$^{-/-}$ E3.5 blastocysts, SRC-1 and PPARγ mRNA levels were strikingly lower when compared to PIMT$^{+/+}$ blastocysts (Fig. 6B). Reduction in PPARγ mRNA expression in PIMT$^{-/-}$ E3.5 blastocysts suggests that this lipogenic transcription factor may be critical for the early embryonic survival and blastocyst expansion. A modest decrease in PRIP mRNA expression and an increase in CBP expression in PIMT$^{-/-}$ E3.5 blastocysts was noted (Fig. 6B). It should be noted that PRIP null mutation has been shown to be embryonic lethal at midgestational development (E10.5-E12.5) (Kuang et al., 2002; Mahajan and Samuels, 2008; Zhu et al., 2003). These observations suggest that PRIP and PRIP-interacting protein PIMT are vital to early embryonic development.

2.7. PIMT-deficiency induces apoptotic cell death in blastocyst cells

Freshly isolated homozygous PIMT$^{-/-}$ E3.5 blastocysts were morphologically discernible from their wild-type (PIMT$^{+/+}$) counterparts (Fig. 7A,B). As pointed out above, increased nuclear fragmentation, suggestive of apoptotic changes, was evident in freshly isolated DAPI stained PIMT deficient blastocysts (Fig. 5C). We confirmed increased apoptotic activity in PIMT$^{-/-}$ blastocysts when they were examined for DNA fragmentation by TUNEL assay (Fig. 7A). TUNEL positive apoptotic cells were frequently seen in PIMT$^{-/-}$ blastocysts (Fig. 7A). PIMT$^{-/-}$ E3.5 day blastocysts when cultured in vitro for 1- to 4 days displayed severely impaired proliferation and reduced number of nuclei when stained by SYTO16, a novel highly sensitive nucleic acid stain to vitally stain DNA (Fig. 7B). We noted that PIMT-null blastocysts did not efficiently adhere to 0.1% gelatin coated 24-well plates and a majority of these did not normally hatch from their zona pellucida (Fig. 7C). PIMT$^{-/-}$ blastocysts remained mostly unhatched with intact zona pellucida at the time of hatching of the wild-type blastocysts, usually by E3.5+2 days pellucida (Fig. 7C). PIMT null blastocysts were smaller and appeared condensed after 24 h (E3.5+1 day) and 48 h (E3.5+2

days) in culture (Fig. 7C). These collapsed and blebbed blastocysts showed no expansion of ICM even at the end of 4 days in culture (not shown). PIMT$^{-/-}$ blastocysts, when hatched, showed growth retardation and failed to develop ICM in contrast to the robust growth of this structure in the wild-type (PIMT$^{+/+}$) embryos (Fig. 7C). These results indicate that the disruption of *PIMT* gene leads to early embryonic lethality at around blastocyst stage. This may be due to abnormalities in the transcription of crucial genes and also to defects in RNA methylation. PIMT protein has been shown to interact with transcription cofactors, bind RNA and exhibit RNA methyltransferase activity (Komonyi et al., 2005; Mouaikel et al., 2002; Zhu et al., 2001). Subsequently, it has been shown that methyltransferase activity of PIMT/Tgs1 is responsible for the hypermethylation of the 5′ m^{7}G cap structure of snRNAs and snoRNAs (Mouaikel et al., 2002). PIMT/Tgs1 has been shown recently to participate in telomerase RNA biogenesis (Tang et al., 2012). These properties, coupled with very early expression of this protein, even at the 2-cell stage embryos (Evsikov et al., 2004; Hamatani et al., 2004), with abnormalities in blastocyst progression, suggest that this protein might interfere with transcription of critical genes and RNA processing during cell proliferation.

2.8. PIMT$^{-/-}$ MEFs show defective wound healing and cell cycle arrest

In view of the failure of expansion of PIMT$^{-/-}$ blastocysts, we decided to generate PIMT deficient MEFs to confirm that PIMT is essential for cell proliferation. We used these MEFs for assaying in vitro wound healing because cell migration and proliferation are prominent components of this process. Fibroblast motility was assessed by a scratch-induced wound healing assay (Fig. 8A-D). MEFs from PIMT$^{flox/flox}$ embryos were cultured to form a near confluent monolayer and migration monitored for 24 h in a scratch wound assay (Fig. 8A,B). To assess the role of PIMT deletion, the cells were infected with adeno-Cre at the time of wounding (Fig. 8C,D) to delete PIMT and the healing compared with uninfected MEFs (Fig. 8A,B) and MEFs infected with Ad-LacZ virus (not shown). PIMT gene deletion was confirmed by PCR genotyping (Fig. 8E). RT-PCR assay was used to ascertain the deletion of exons 3 and 4 with primers designed from the exons 2 and 5 (Fig. 8F). Western blot analysis using polyclonal antibodies (antibody N-13) generated against N-terminal portion of PIMT (aa 1-50) or against an internal region (aa 200-250) (antibody P-12) revealed the presence of PIMT protein in PIMT$^{fl/fl}$ MEFs but not prominent in Ad-Cre treated PIMT$^{fl/fl}$ MEFs (Fig. 8G). Complete wound healing did not occur in PIMT-null MEFs (Fig. 8C,D). These observations clearly establish that PIMT is involved in wound repair. To assess the role of PIMT in fibroblast proliferation, we studied the incorporation of bromodeoxyuridine (BrdUrd) over a 3 hr period in PIMT$^{+/+}$ and PIMT$^{-/-}$ MEFs (Fig. 8H-J). Immunohistochemical staining revealed a reduction in the number of BrdUrd positive cells in PIMT$^{-/-}$ MEFs (26% cells labeled) when compared to PIMT$^{+/+}$ population (70% cells labeled) (Fig. 8H-J). We undertook flow cytometric analysis of MEFs to assess defects in cell cycle, if any, in PIMT deficiency. In PIMT$^{+/+}$ MEFs, 63.8% of cells were in G_0/G_1 phase, 24.0% in S phase, and 12.2% in G_2/M phase. In contrast, MEFs infected with adeno-Cre for 24 h to disrupt PIMT gene revealed 49.2% in G_0/G_1, 19.4% in S phase, and 31.4% in G_2/M phase indicating that PIMT deficiency causes G_2 arrest (data not shown). These observations suggest an important role for PIMT in cell cycle progression.

One important consideration is that the disruption of PIMT gene, by eliminating *N*-terminal amino acids 57-381, interferes with its interaction with coactivator PRIP (Zhu et al., 2001). It is possible that the abolition of this PIMT-PRIP interaction might lead to early embryonic lethality, even if the short-RNA were to encode a truncated PIMT protein. Also worth noting is that the targeting construct was designed to preserve the conserved C-terminal methyltransferase domain (Zhu et al., 2001), and N-terminal consensus G*XX*G (Gly-X-X-Gly) segment found in the K-homology RNA-binding domain (Svitkin et al., 1996; Brykailo et al., 2007). If the truncated protein was formed and functionally intact, the findings

reported here suggest that the embryonic lethality does not depend on the presence or absence of the methyltransferase activity of PIMT. We conclude that the removal of the PRIP-interacting upstream region (exons 3 and 4) of PIMT is sufficient to cause the early embryonic lethality. Further analysis of the various functional domains of PIMT appears necessary to understand the embryonic mortality resulting from the disruption of this gene.

Disruption of some coactivator genes, such as MED1 and NCoA6, has been shown to result in embryonic lethality mostly around E10.5 through E12.5 (Ito et al.,2000; Mahajan and Samuels, 2008; Zhu et al., 2000a, 2003), whereas disruption of genes encoding p160/SRC family of proteins in the mouse results in a viable phenotype (Lonard and O'Malley, 2006; Reddy et al., 2006; Yu and Reddy, 2007; Wang et al., 2006). In contrast, PIMT gene disruption causes early embryonic lethality as E3.5 $PIMT^{-/-}$ blastocysts are defective and generally failed hatch from the zona pellucida, as described with other "essential" genes (Forschegger et al., 2007; Wilson et al., 2007). PIMT appears to be an essential gene in early development of blastocyst as who by apoptosis and reduced cell number if PIMT deficient E3.5 day blastcyst. Of interest is the finding that PIMT null blastocysts exhibit marked reduction in Oct4 and Nanog immunofluorescence. Further studies will be necessary to examine the relationship between PIMT and the key transcription factors involved in the development of ICM. It is possible that PIMT is essential for RNA metabolism and cell cycle progression in addition to some unknown functions in transcription. Also of interest is that mice with PIMT floxed alleles generated here would enable serve as a model to examine the role of this coactivator in cell specific functions.

3. Experimental procedures

3.1. Phylogenetic analysis and evolution of PIMT gene

The amino acid sequences from the open reading frames were initially aligned using the program ClustalW2. Conserved motifs containing RNA methyltransferase domains from ten species were used for this alignment (Zhu et al., 2001). These alignments were then reconciled and further adjusted manually to minimize insertion/deletion events. The conserved motifs were defined as alignable regions among all sequences. Smaller groups of more closely related sequences were then aligned separately by the same approach. Only regions of unambiguous alignments were used in the subsequent phylogenetic analyses. Phylogenetic tree was inferred by the neighbor joining functionality of ClustalW (Saito and Nei, 1987). Tree was constructed using alignable amino acids from sixteen species using ClustalW and manually edited. Column containing gaps were deleted and bootstrap analyses consisted of 1000 replicates using neighbor joining method.

3.2. Histology and immunohistochemistry

Mouse embryos and E3.5 blastocysts were fixed in 4% paraformaldehyde in phosphate buffered saline for 16 h at 4°C. The embryos were dehydrated in graded alcohols, embedded in paraffin, sectioned at 4 μm, and stained with hematoxylin and eosin. Sections were also processed for immunohistochemical localization of PIMT using polyclonal PIMT antibodies (Santa Cruz Biotechnology Inc.). Whole-mount immunostaining was performed on balstocysts using antibodies against Nanog, Oct4, Cdx2 and PIMT (Santa Cruz Biotechnology Inc.), photographed with confocal microscopy. For incorporation of bromodeoxyuridine (BrdUrd) in $PIMT^{+/+}$ and $PIMT^{-/-}$ MEFs, cells were labeled for 3 hr by supplementation of the culture medium with BrdUrd (Sigma; St Louis. MO; 10 μM). After the labeling, the cultures were rinsed in PBS and the cells were suspended with 0.05% Trypsin EDTA. The MEFs suspension centrifuged onto glass slides with cytocentrifuge. The cytocentrifuge preparations were fixed for 10 min in 90% ethanol in distilled water, followed immediately by 4% paraformaldehyde in PBS. Using mouse monoclonal BrdUrd

antibody(BD). All animal procedures used in this study were reviewed and pre-approved by the Institutional Review Boards for Animal Research of the Northwestern University.

3. 3 Immunoblot Analysis

For immunoblotting, total protein from mouse embryos (E10.5 – E18.5) and from PIMT+/+ and PIMT−/− MEFs were extracted and processed using antibodies against PIMT (N-13 and P-12, Santa Cruz Biotechnology Inc.) and antibody against ß-actin (Santa Cruz Biotechnology Inc.) as a loading control. PIMT protein synthesized by in vitro translation using the TnT-coupled transcription- translation system (Promega) was used as a positive control.

3.4. RT-PCR and Q-PCR analysis

The SuperScript III CellsDirect cDNA Synthesis System Invitrogen) was used for synthesizing first-strand cDNA directly from the preimplantation embryo lysate. Single embryos were resuspended in the lysis buffer, treated with DnaseI and reverse transcribed in the same tube. The same cDNA was used as a template for the quantitative PCR. All of the primers were synthesized by Integrated DNA Technologies (Coralville, IA, USA). β-Actin was used as a RNA loading control for the RT-PCR, whereas 18 S rRNA was used as an internal control for the quantitative PCR.

3.5. Gene-targeting and homologous recombination in ES cells

A BAC containing the genomic PIMT locus, 7A17, was identified by screening high density BAC library derived from a 129S6/SvEvTac mouse (Invitrogen). A gene-targeting vector, designed to delete PIMT exons 3 and 4, included two-*loxP* and two-*frt* cis-elements. A cassette harboring frt-*neo*-*frt*-*loxP* (~2.1 kb) was retrieved from the pDELBOY and inserted into the XhoI and KpnI site of pBluescript (SK+). A 2.3-kilobase PCR fragment containing intron 2 to 3 served as a 5′-homology arm while 2.0 kb intron 4 was used as 3′-homology arm for the recombination. The final targeting construct was designated mPIMT-KO. The *Not*I-linearized targeting vector (40 μg) was electroporated into HM1 embryonic stem (ES) cells and selected in a medium containing 200 μg/ml G418 and 2 μM ganciclovir. Surviving colonies were screened for homologous recombination event by PCR using forward (designed in the second LoxP): 5′-GACGCGTATAACTTCGTATAGCATAC-3′ and reverse (designed out of the 3′ homology arm): 5′-GCATGTGAGTACACTGCTGC-3′ primers. Four positive ES cell clones were found among 248 screened and confirmed by Southern blot analysis.

3.6. Generation of PIMT knockout mice

Euploid selected ES cells were used for injection into 3.5 day old blastocysts derived from C57BL/6J mouse to obtain chimeric mice. Chimeric male mice were bred with wild-type C57BL/6J female to produce heterozygous mice. After successful germ line transmission, PIMTfl/fl-frt-neo-frt mice were crossed with FLP1 recombinase variant (FLPeR) transgenic deleter mice (Jackson Laboratory) to facilitate in vivo *frt*-mediated *neo* deletion. The $PIMT^{flox/flox}$ mice were further crossed with EIIa-Cre (adenovirus EIIa promoter driving Cre recombinase) transgenic mice (Jackson Laboratory) to generate $PIMT^{-/-}$ mice. Mice were genotyped by PCR followed by Southern blotting using a 1.0 kb probe amplified from the intronic 4 region of PIMT genomic locus. Electroporation and blastocyst injections were done by the Transgenic and Targeted Mutagenesis Laboratory of the Northwestern University.

3.7. Genotyping

DNA obtained from the tail tips of 3-week-old mice and from laser catapult microdissected embryos at E5.5 and E6.5 was genotyped by PCR amplification using three primers P4/P5/P6 in the same reaction to detect the targeted and wild type allele. The results were confirmed by Southern blotting. For 3.5-day embryo genotyping, blastocysts were flushed out of uterus, washed with water, and then transferred into tubes containing 10 μl of water and 7 μl of phosphate buffered saline. DNA from blastocysts was released by successive dry ice-freezing and boiling steps followed by 30-min incubation at 56°C in the presence of 3 μl of proteinase K (10 mg/ml). A final incubation was done at 95°C for 10 min, and samples were kept at −20°C. The lysate was used for a first round PCR using three primers P1/P2/P3 followed by nested PCR with the primers P4/P5/P6 under standard conditions. The primers consisted of P1: 5′-GTTCATCTTAGACTCTCCAGCTTC-3′, P2: 5′-CCAAGACAGAGGCATCAAGAATAT-3′, P3: 5′-GGAGACCTCAGTCTGCTTAACAC-3′, P4: 5′-CTGCATGTATGAATCTTGGGAG-3′, P5: 5′-GCATCAAGAATATACAGAACAGAGA CTC-3′ and P6: 5′-CTCCTTCCTTCTGTACCTCTGTAGC-3′.

3.8. Blastocyst culture

Superovulated heterozygous $PIMT^{+/-}$ females were crossed with heterozygous $PIMT^{+/-}$ males. Superovulation was induced by i.p. injection of 5 IU of pregnant mare serum gonadotropin, followed 48 h later by 5 IU of human chorionic gonadotropin. Successful mating was confirmed by the presence of a vaginal plug and its presence was scored as gestation day E0.5 (0.5 post-coitum or 0.5 pc). Blastocysts were collected at embryonic day 3.5 (E3.5) by flushing uteri with ES cell medium (Fortschegger et al., 2007; Hyenne et al., 2007; Li et al., 2004; Wilson et al., 2007). For in vitro culture, blastocysts were placed individually for 3.5 days in ES cell medium in 0.1% gelatin coated 24-well plates and photographed every 24 h using an Axiovert phase-contrast microscope (Zeiss).

3.9. TUNEL assay and vital staining of nuclei

Apoptosis was determined by terminal deoxynucleotidyl transferase (TdT) mediated dUTP nick end labeling (TUNEL) staining, using In Situ Cell Death Detection kit (Roche Diagnostics Corp.). Harvested E3.5 blastocysts were cultured in ES cell medium for 24 h, fixed in 4% paraformaldehyde-PBS for 1 h, and permeabilized in 0.5% Triton X-100 for 30 min, then the blastocysts were incubated with TdT and fluorescence labeled dUTP reaction mixture at 37 °C for 1 h. After nuclear DNA staining with 1 μg/ml DAPI in PBS, the blastocysts were examined by light and fluorescence microscopy. For nuclear number, individual blastocysts were cultured in the presence of 1 μM SYTO16 (Invitrogen) to vitally stain DNA for 24 h and photographed using phase contrast and fluorescence microscopy (Wilson et al., 2007; Yuba-Kubo et al., 2005). These blastocysts were then genotyped by PCR amplification as described above.

3.10. Generation of $PIMT^{-/-}$ MEFs- $PIMT^{flox/flox}$

MEFs were derived from individual 12.5 day-old $PIMT^{flox/flox}$ embryos and grown in Dulbecco's Modified Eagle's Medium with 10% (vol/vol) heat-inactivated fetal bovine serum supplemented with 2 mM L-glutamine, 50 units/ml penicillin and 50 μg/ml streptomycin (Hyclone). Cultures were incubated at 37°C with 5% CO_2 and passaged two times a week. To delete the floxed PIMT alleles for the generation of $PIMT^{-/-}$ MEFs, the PIMT $^{flox/flox}$ MEFs were infected with 2.5, 5 or 7.5 μl (0. 8×10^{13} VP/ml) of a recombinant adenovirus expressing the Cre recombinase (Ad/Cre). Deletion of PIMT gene in MEFs following Ad/Cre infection was confirmed by PCR analysis using primers P1 through P6 as described above. RT-PCR was used to ascertain the deletion of exons 3 and 4.

3.11. Cell migration and wound healing

Migration of $PIMT^{+/+}$ and $PIMT^{-/-}$ MEFs was monitored over 48 h using a scratch wound assay (Matsumoto et al., 2007). Linear scrape wounds were made in subconfluent monolayers of MEFs by using a pipette tip to make a uniform scratch along the tissue culture plate. They were allowed to heal for 24 h in serum-free medium. For flow cytometric analysis, MEFs were stained with propidium iodide (Invitrogen), and fluorescence was measured using a Beckman Coulter XL100 flow cytometer equipped with a 488-nm laser and the data analyzed using Modfit software (Verity Software House, Topsham, ME).

Acknowledgments

This work was supported, in part, by grants from the National Institutes of Health Grants DK083163 (to J. K. R.), and DK60635 (Y.S.K.). The authors thank Philip F. Fitchev, Sean Pyper, R. Zaak Walton, Chao Qi, Lynn Doglio and Warren Tourtellotte for their assistance and discussion in the technical aspects of the work.

REFERENCES

Auboeuf D, Dowhan DH, Dutertre M, Martin N, Berget SM, O'Malley BW. A Subset of Nuclear Receptor Coregulators Act as Coupling Proteins during Synthesis and Maturation of RNA Transcripts. Mol. Cell. Biol. 2005; 25:5307–5316. [PubMed: 15964789]

Brykailo MA, Corbett AH, Fridovich-Keil JL. Functional overlap between conserved and diverged KH domains in Saccharomyces cerevisiae SCP160. Nucleic Acids Res. 2007; 35:1108–1118. [PubMed: 17264125]

Chambers I, Colby D, Robertson M, Nichols J, Lee S, Tweedie S, Smith A. Functional expression cloning of Nanog, a pluripotency sustaining factor in embryonic stem cells. Cell. 2003; 113:643–655. [PubMed: 12787505]

Chazaud C, Yamanaka Y, Pawson T, Rossant J. Early lineage segregation between epiblast and primitive endoderm in mouse blastocysts through the Grb2-MAPK pathway. Dev Cell. 2006; 10:615–624. [PubMed: 16678776]

Cho Y-W, Hong T, Hong SH, Guo H, Yu H, Kim D, Guszczynski T, Dressler GR, Copeland TD, Kalkum M, Ge K. PTIP associates with MLL3- and MLL4 containing histone H3 lysine 4 methyltransferase complex. J. Biol. Chem. 2007; 282:20395–20406. [PubMed: 17500065]

Conaway JW, Florens L, Sato S, Tomomori-Sato C, Parmely TJ, Yao T, Swanson SK, Banks CAS, Washburn MP, Conaway RC. The mammalian Mediator complex. FEBS Letters. 2005; 579:904–908. [PubMed: 15680972]

Crawford SE, Qi C, Misra P, Stellmach V, Rao MS, Engel JD, Zhu Y, Reddy JK. Defects of the heart, eye, and megakaryocytes, in peroxisome proliferator activator receptor-binding protein (PBP) null embryos implicate GATA family of transcription factors. J Biol Chem. 2002; 277:3585–3592. [PubMed: 11724781]

Enunlu I, Papai G, Cserpan I, Udvardy A, Jeang K-T, Boros I. Different isoforms of PRIP-interacting protein with methyltransferase domain/trimethylguanosine synthase localizes to the cytoplasm and nucleus. Biochem. Biophys. Res. Commun. 2003; 309:44–51. [PubMed: 12943661]

Evsikov AV, de Vries WN, Peaston AE, Radford EE, Fancher KS, Chen FH, Blake JA, Bult CJ, Latham KE, Solter D, Knowles BB. Systems biology of the 2-cell mouse embryo. Cytogenet. Genome, Res. 2004; 105:240–250. [PubMed: 15237213]

Fondell JD, Ge H, Roeder RG. Ligand induction of a transcriptionally active thyroid hormone receptor coactivator complex. Proc Natl Acad Sci U S A. 1996; 93:8329–8933. [PubMed: 8710870]

Fortschegger K, Wagner B, Voglauer R, Katinger H, Sibilia M, Grillari J. Early embryonic lethality of mice lacking the essential protein SNEV. Mol. Cell. Biol. 2007; 27:3123–3130. [PubMed: 17283042]

Gasperowicz M, Natale DR. Establishing three blastocyst lineages--then what? Biol Reprod. 2011; 84:621–630. [PubMed: 21123814]

Girard C, Verheggen C, Neel H, Cammas A, Vagner S, Soret J, Bertrand E, Bordonne R. Characterization of a short isoform of human Tgs1 hypermethylase associating with small

nucleolar ribonucleoprotein core proteins and produced by limited proteolytic processing. J. Biol. Chem. 2008; 283:2060–2069. [PubMed: 18039666]

Hamatani T, Carter MG, Sharov AA, Ko MS. Dynamics of global gene expression changes during mouse preimplantation development. Dev Cell. 2004; 6:117–31. [PubMed: 14723852]

Hermanson O, Glass CK, Rosenfeld MG. Dynamics of global gene expression changes during mouse preimplantation development. Trends Endocrinol. Metabol. 2002; 13:55–60.

Hyenne V, Souilhol C, Cohen-Tannoudji M, Cereghini S, Petit C, Langa F, Maro B, Simmler MC. Conditional knock-out reveals that zygotic vezatin-null mouse embryos die at implantation. Mech. Dev. 2007; 124:449–462. [PubMed: 17452094]

Ito M, Yuan CX, Okano HJ, Carnell RB, Roeder RG. Involvement of the TRAP220 component of the TRAP/SMCC coactivator complex in embryonic development and thyroid hormone action. Mol. Cell. 2000; 5:683–693. [PubMed: 10882104]

Jia Y, Qi C, Kashireddi P, Surapureddi S, Zhu YJ, Rao MS, Le Roith D, Chambon P, Gonzalez FJ, Reddy JK. Transcription coactivator PBP, the peroxisome proliferator-activated receptor (PPAR)-binding protein, is required for PPARα-regulated gene expression in liver. J. Biol. Chem. 2004; 279:24427–24434. [PubMed: 15150259]

Jia Y, Guo GL, Surapureddi S, Sarkar J, Qi C, Guo D, Xia J, Kashireddi P, Yu S, Cho YW, Rao MS, Kemper B, Ge K, Gonzalez FJ, Reddy JK. Transcription coactivator peroxisome proliferator-activated receptor-binding protein/mediator 1 deficiency abrogates acetaminophen hepatotoxicity. Proc. Natl. Acad. Sci. U. S. A. 2005; 102:12531–12536. [PubMed: 16109766]

Komonyi O, Papai G, Enunlu I, Muratoglu S, Pankotai T, Kopitova D, Maróy P, Udvardy A, Boros I. DTL, the Drosophila homolog of PIMT /Tgs1 nuclear receptor coactivator interacting protein / RNA methyltransferase, has an essential role in development. J. Biol. Chem. 2005; 280:12397–12404. [PubMed: 15684427]

Kornberg RD. The molecular basis of eukaryotic transcription. Proc. Natl. Acad. Sci. U.S.A. 2007; 104:12955–12961. [PubMed: 17670940]

Kuang SQ, Liao L, Zhang H, Pereira FA, Yuan Y, Demayo FJ, Ko L, Xu J. Deletion of the cancer-amplified coactivator AIB3 results in defective placentation and embryonic lethality. J. Biol. Chem. 2002; 277:45356–45360. [PubMed: 12368298]

Lemon B, Inouye C, King DS, Tjian R. Selectivity of chromatin-remodelling cofactors for ligand-activated transcription. Nature. 2001; 414:924–928. [PubMed: 11780067]

Lewis BA, Reinberg D. The mediator coactivator complex: functional and physical roles in transcriptional regulation. J. Cell Sci. 2003; 116:3667–3675. [PubMed: 12917354]

Li T, Inoue A, Lahti JM, Kidd VJ. Failure to proliferate and mitotic arrest of CDK11p110/p58-null mutant mice at the blastocyst stage of embryonic cell development. Mol. Cell. Biol. 2004; 24:3188–3197. [PubMed: 15060143]

Lonard DM, O'Malley BW. The expanding cosmos of nuclear receptor coactivators. Cell. 2006; 125:411–414. [PubMed: 16678083]

Mahajan MA, Samuels HH. Nuclear receptor coactivator/coregulator NCoA6 (NRC) is a pleiotropic coregulator involved in transcription, cell survival, growth and development. Nucl. Recep. Signaling. 2008; 6:1–19.

Matsumoto K, Yu S, Jia Y, Ahmed MR, Viswakarma N, Sarkar J, Kashireddy PV, Rao M,S, Karpus W, Gonzalez FJ, Reddy JK. Critical role for transcription coactivator peroixsome proliferator-activated receptor PPAR)-binding protein TRAP/220 in liver regeneration and PPARα ligand-induced liver tumor development. J. Biol. Chem. 2007; 282:17053–17060. [PubMed: 17438330]

Misra P, Qi C, Yu S, Shah SH, Cao W-Q, Rao MS, Thimmapaya B, Zhu Y, Reddy JK. Interaction of PIMT with Transcriptional Coactivators CBP, p300, and PBP Differential Role in Transcriptional Regulation. J. Biol. Chem. 2002; 277:20011–20019. [PubMed: 11912212]

Mitsui K, Tokuzawa Y, Itoh H, Segawa K, Murakami M, Takahashi K, Maruyama M, Maeda M, Yamanaka S. The homeoprotein Nanog is required for maintenance of pluripotency in mouse epiblast and ES cells. Cell. 2003; 113:631–642. [PubMed: 12787504]

Mouaikel J, Verheggen C, Bertrand E, Tazi J, Bordonne R. Hypermethylation of the cap structure of both yeast snRNAs and snoRNAs requires a conserved methyltransferase that is localized to the nucleolus. Mol. Cell. 2002; 9:891–901. [PubMed: 11983179]

Nichols J, Zevnik B, Anastassiadis K, Niwa H, Klewe-Nebenius D, Chambers I, Schöler H, Smith A. Formation of pluripotent stem cells in the mammalian embryo depends on the POU transcription factor Oct4. Cell. 1998; 95:379–391. [PubMed: 9814708]

Onate SA, Tsai SY, Tsai MJ, O'Malley BW. Sequence and characterization of a coactivator for the steroid hormone receptor superfamily. Science. 1995; 270:1354–1357. [PubMed: 7481822]

Rachez C, Lemon BD, Suldan Z, Bromleigh V, Gamble M, Naar AM, Erdjument-Bromage H, Tempst P, Freedman LP. Ligand-dependent transcription activation by nuclear receptors requires the DRIP complex. Nature. 1999; 398:824–828. [PubMed: 10235266]

Reddy JK, Guo D, Jia Y, Yu S, Rao MS. Nuclear receptor transcriptional coactivators in development and metabolism. Adv. Dev. Biol. 2006; 16:389–420.

Roeder RG. Transcriptional regulation and the role of diverse coactivators in animal cells. FEBS Lett. 2005; 579:909–915. [PubMed: 15680973]

Rossant J, Tam PPL. Blastocyst lineage formation, early embryonic asymmetries and axis patterning in the mouse. Development. 2009; 136:701–713. [PubMed: 19201946]

Saitou N, Nei M. The neighbor-joining method: a new method for reconstructing phylogenetic trees. Mo. Biol. Evol. 1987; 4:406–425.

Shang Y, Hu X, DiRenzo J, Lazar MA, Brown M. Cofactor dynamics and sufficiency in estrogen receptor-regulated transcription. Cell. 2000; 103:843–852. [PubMed: 11136970]

Spiegelman BM, Heinrich R. Biological control through regulated transcriptional coactivators. Cell. 2004; 119:157–167. [PubMed: 15479634]

Surapureddi S, Yu S, Bu H, Hashimoto T, Yeldandi AV, Kashireddy P, Cherkaoui-Malki M, Qi C, Zhu YJ, Rao MS, Reddy JK. Identification of a transcriptionally active peroxisome proliferator-activated receptor alpha-interacting cofactor complex in rat liver and characterization of PRIC285 as a coactivator. Proc. Natl. Acad. Sci. U. S. A. 2002; 99:11836–11841. [PubMed: 12189208]

Svitkin YV, Ovchinnikov LP, Dreyfus G, Sonenbrg N. General RNA binding proteins render translation cap dependent. The EMBO J. 1996; 15:7147–7155.

Tang W, Kannan R, Blanchette M, Baumann P. Telomerase RNA biogenesisi involves sequential binding by Sm and Lsm complexes. Nature. 2012; 484:260–264. [PubMed: 22446625]

Verheggen C, Bertrand E. CRM1 plays a nuclear role in transporting snoRNPs to nucleoli in higher eukaryotes. Nucleus. 2012; 3(2) 1.

Viswakarma N, Jia Y, Bai L, Vluggens A, Borensztajn J, Xu J, Reddy JK. Coactivators in PPAR-Regulated Gene Expression. PPAR Res. 2010; 2010(pii):250126. [PubMed: 20814439]

Wang Z, Qi C, Krones A, Woodring P, Zhu X, Reddy JK, Evans RM, Rosenfeld MG, Hunter T. Critical roles of the p160 transcriptional coactivators p/CIP and SRC-1 in energy balance. Cell Metab. 2006; 3:111–122. [PubMed: 16459312]

Wilson MD, Wang D, Wagner R, Breyssens H, Gertsenstein M, Lobe C, Lu X, Nagy A, Burke RD, Koop BF, Howard PL. ARS2 is a conserved eukaryotic gene essential for early mammalian development. Mol. Cell. Biol. 2007; 28:1503–1514. [PubMed: 18086880]

Xu J, Liao L, Ning G, Yoshida-Komiya H, Deng C, O'Malley BW. The steroid receptor coactivator SRC-3 (p/CIP/RAC3/AIB1/ACTR/TRAM-1) is required for normal growth, puberty, female reproductive function, and mammary gland development. Proc. Natl. Acad. Sci. U. S. A. 2000; 97:6379–6384. [PubMed: 10823921]

Yadavalli VSRK, Jeang K-T. Trinethylguanosine capping selectively promotes expression of Rev-dependeent HIV-1 RNAs. Proc. Natl. Acad. Sci. U. S. A. 2010; 107:14787–14792. [PubMed: 20679221]

Yu S, Reddy JK. Transcriptiojn coactivators for peroxisome proliferator-activated receptors. Biochim. Biophys. Acta. 2007; 1771:936–951. [PubMed: 17306620]

Yuan CX, Ito M, Fondell JD, Fu ZY, Roeder RG. The TRAP220 component of a thyroid hormone receptor- associated protein (TRAP) coactivator complex interacts directly with nuclear receptors in a ligand-dependent fashion. Proc. Natl. Acad. Sci. U. S. A. 1998; 95:7939–7944. [PubMed: 9653119]

Yuba-Kubo A, Kubo A, Hata M, Tsukita S. Gene knockout analysis of two γ–tubulin isoforms in mice. Dev. Biol. 2005; 282:361–373. [PubMed: 15893303]

Zhu YJ, Crawford SE, Stellmach V, Dwivedi RS, Rao MS, Gonzalez FJ, Qi C, Reddy JK. Coactivator PRIP, the peroxisome proliferator-activated receptor-interacting protein, is a modulator of placental, cardiac, hepatic, and embryonic development. J. Biol. Chem. 2003; 278:1986–1990. [PubMed: 12446700]

Zhu Y, Qi C, Jia Y, Nye JS, Rao MS, Reddy JK. Deletion of PBP/PPARBP, the gene for nuclear receptor coactivator peroxisome proliferator-activated receptor-binding protein, results in embryonic lethality. J. Biol. Chem. 2000a; 275:14779–14782. [PubMed: 10747854]

Zhu Y, Kan L, Qi C, Kanwar YS, Yeldandi AV, Rao MS, Reddy JK. Isolation and characterization of peroxisome proliferator-activated receptor (PPAR) interacting protein (PRIP) as a coactivator for PPAR. J. Biol. Chem. 2000b; 275:13510–13516. [PubMed: 10788465]

Zhu Y, Qi C, Cao WQ, Yeldandi AV, Rao MS, Reddy JK. Cloning and characterization of PIMT, a protein with a methyltransferase domain, which interacts with and enhances nuclear receptor coactivator PRIP function. Proc. Natl. Acad. Sci. U. S. A. 2001; 98:10380–10385. [PubMed: 11517327]

Zhu Y, Qi C, Jain S, Rao MS, Reddy JK. Isolation and characterization of PBP, a protein that interacts with Peroxisome Proliferator-activated Receptor. J. Biol. Chem. 1997; 272:25500–25506. [PubMed: 9325263]

Highlights

- PIMT (NCOA6IP/Tgs1), a RNA-binding protein with RNA methyltransferase activity, is a conserved protein with dual critical cellular functions in that it serves as a transcription cofactor and as trimethylguanosine synthase.
- PIMT is expressed in all cells of the 3.5 day mouse blastocyst.
- Disruption of the PIMT gene is associated with reduction of Oct4 and Nanog proteins resulting in impairment of ICM formation and early embryonic lethality in the mouse.
- PIMT deficient mouse embryos die at the time of implantation and then resorbed.
- PIMT deficiency results in a reduction in G_0/G_1 transition and G_2/M cell cycle arrest.

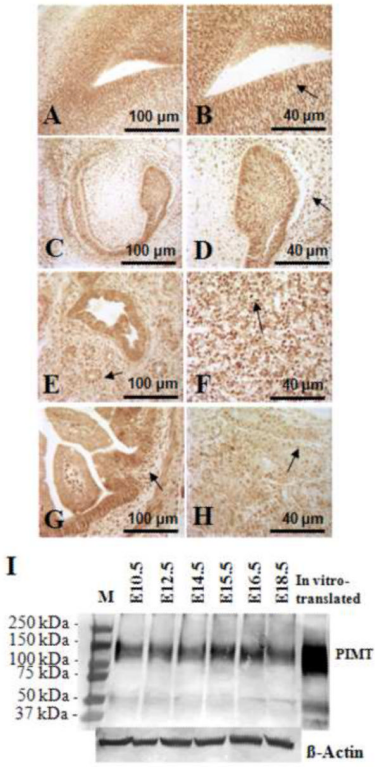

Fig. 1.

Immunohistochemical localization and western blotting for PIMT in mouse embryo. (A-H) Wild-type $PIMT^{fl/fl}$ E16.5 embryo processed for light microscopy. De-paraffinized 4-5 μM thick sections were immunohistochemically stained using PIMT antibody. PIMT expression is evident in the lateral ventricle of the brain (A, B), enamel bud (C, D), lung (E), liver (F), intestinal mucosal crypts (G), and testis (H). PIMT is predominantly localized in the nucleus (*arrows*). (I) PIMT protein expression was analyzed by immunoblotting of total body homogenates derived from E10.5, E12.5, E14.5, E16.5 and E18.5 mouse embryos, using anti-PIMT antibody. PIMT protein was confirmed as a ~ 110 kDa band using in-vitro translated PIMT as a positive control. Equal loading of protein was confirmed using antibody against ß-actin.

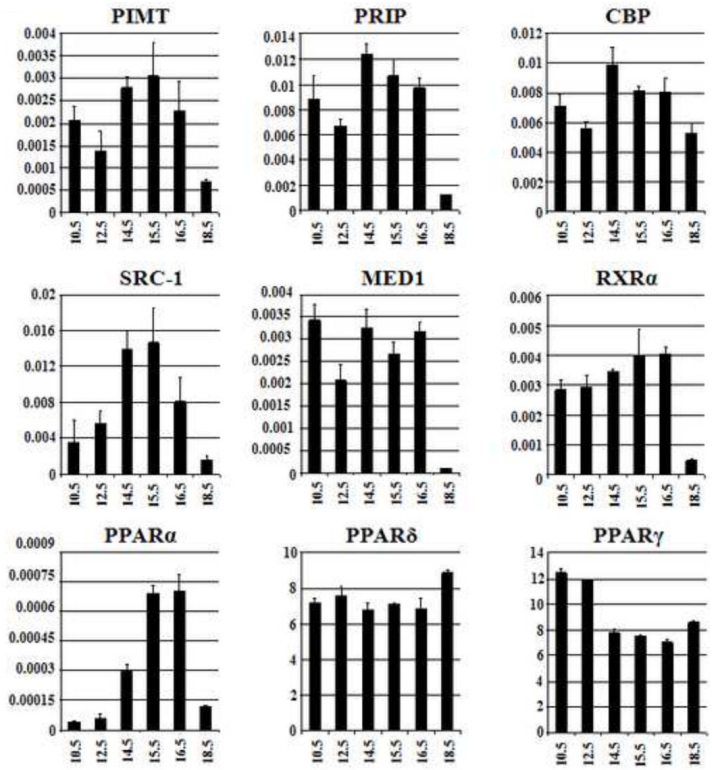

Fig. 2.

Expression of PIMT and other cofactor mRNAs in wild-type developing mouse embryos. The cDNA synthesized using pooled RNA from at least 3 wild-type embryos for each time point (E10.5 to E18.5 days; x axis) was used in Q-PCR to evaluate the expression level of selected coactivators associated with PIMT and some nuclear receptors. Expression levels of PIMT, PRIP, CBP, SRC-1, MED1, RXRα, PPARα, PPARδ and PPARγ are shown. Q-PCR reactions were performed in triplicate and 18 S rRNA was used as an internal control. Error bars indicate standard deviation.

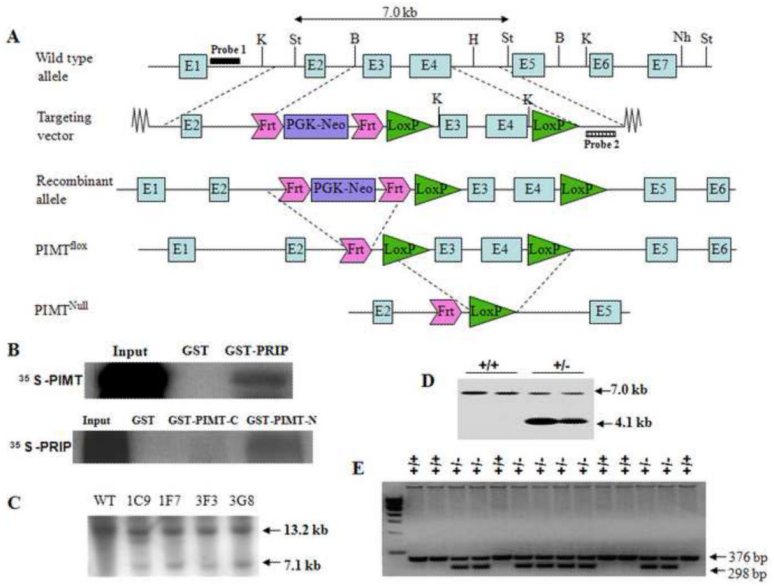

Fig. 3.

Targeting of the PIMT/NCoA6IP locus and genotyping. (A) Strategy for the generation of neomycin (*neo*)-free PIMT null mice by the two-*loxP*, two-*frt* approach. Schematic representation of the mouse PIMT genomic locus, the targeting vector designed to delete PIMT exons 3 and 4 (amino acids 57-381), recombinant and the null allele generated following homologous recombination. The *frt*-flanked *neo* marker was removed from PIMT floxed/floxed mice by crossing them with FLPeR deletor transgenic mice. EIIA-Cre transgenic mice were used to generate germ-line (global) deletion of PIMT gene. Restriction sites KpnI (K), StuI (St), BamHI (B), HindIII (H), NheI (Nh), and the location of the probe used for Southern hybridization are indicated. Dashed lines show the region of homology between the vector and the wild type allele. Location of probes 1 (*dark box*) and 2 (*grided box*) is indicated. (B) PIMT N-terminal portion binds PRIP. Pull-down assay using [^{35}S]-methioine labeled PIMT-N terminal segment (1-369 aa) shows binding to GST-PRIP (773-927 aa). Pull-down assay using [^{35}S]-methionine labeled PRIP reveals no binding to GST-PIMT-C terminal domain (577-852 aa). Binding activity is clearly seen with the N-terminal domain of the protein, while C-terminal binding activity is negligible. (C) Southern blot analysis of genomic DNAs from ES cell clones, designated 1C9, 1F7, 3F3, and 3G8. ES cell DNA digested with KpnI was hybridized with 1.1 kb probe (*grided box*) to show wild type allele (13.2 kb) and recombinant allele (7.1 kb). (D) Southern blot analysis of tail DNA from intercrosses of PIMT$^{+/-}$ mice. Tail DNA was digested with StuI and hybridized with 1.0 kb probe (*dark box*) obtained by amplification from intron 4 of PIMT genomic locus. (E) Genomic DNA from the tail of new born mice derived from PIMT$^{+/-}$ intercrosses. See Fig. 5A for the location of primers used for PCR amplification. Primers P6/P5 yielded a 376 bp wild-type PIMT allele in PIMT$^{+/+}$ mice. Two bands representing 376 bp wild-type, and 298 bp deleted allele were seen in PIMT$^{+/-}$ heterozygous mice amplified using P4, P5 and P6 “nested” primers. No PIMT$^{-/-}$ homozygous deletion was observed.

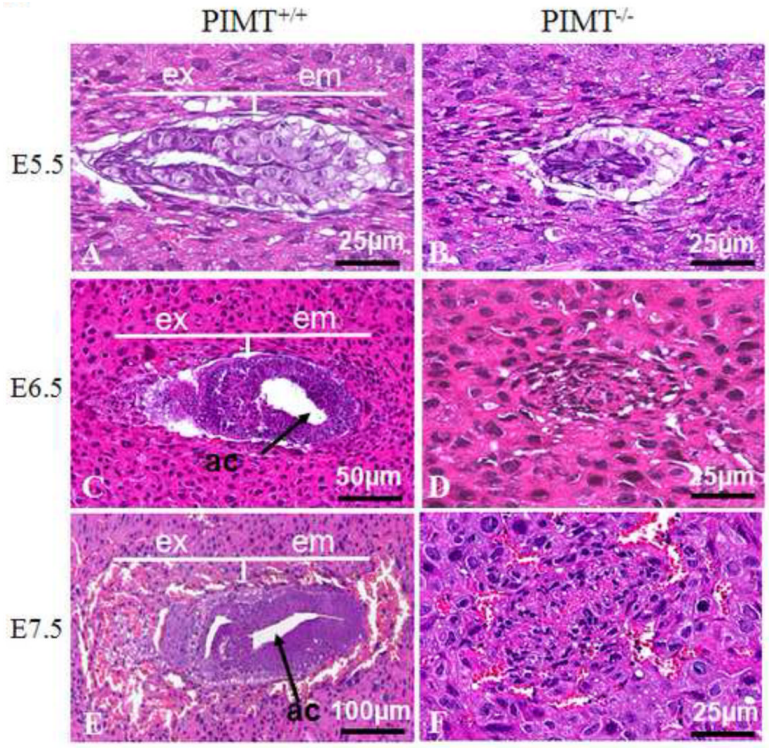

Fig. 4.

Postimplantation development of PIMT$^{-/-}$ embryos. Histological appearance of representative decidual sites from PIMT$^{+/-}$ intercrosses at E5.5, E6.5 and E7.5. Normal deciduae (PIMT$^{+/+}$) contain a normally developed embryo. Developmental arrest and eventual resorption of PIMT$^{-/-}$ embryos. Pyknotic/ apoptotic cells are evident in PIMT null implantation sites. Presumptive E7.5 PIMT null implantation site reveals resorption of embryo. ex, extraembryonic; em, embryo; ac, amniotic cavity.

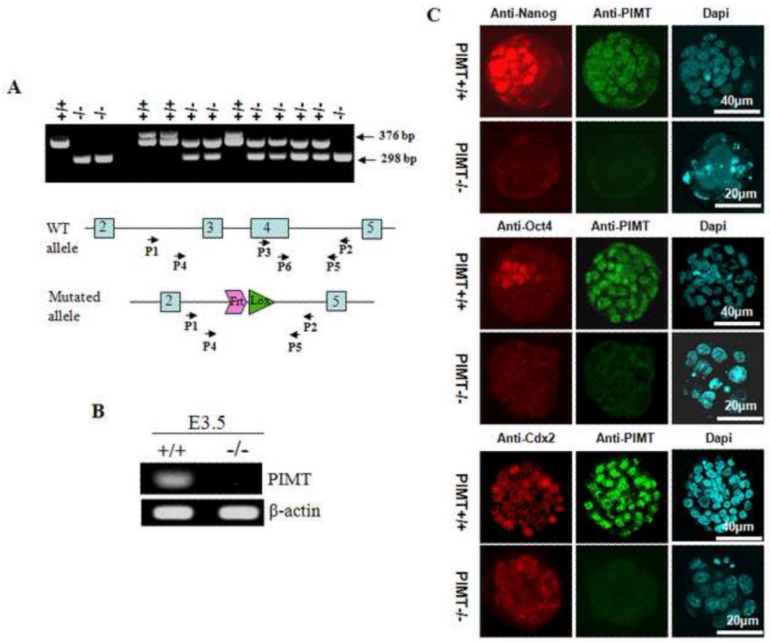

Fig. 5.

Genotyping of blastocysts and PIMT expression. (A) Blastocyst genomic DNA amplification and schematic location of primers used. DNA was isolated from blastocysts derived from $PIMT^{+/-}$ intercrosses at E3.5. Primers P6/P5 yielded a 376 bp wild-type PIMT allele in $PIMT^{+/+}$ blastocysts. Two bands representing 376 bp wild-type, and 298 bp deleted allele were seen in $PIMT^{+/-}$ blastocysts amplified using P4, P5 and P6 "nested" primers. PCR amplification with P4 and P5 generated only a 298 bp product in $PIMT^{-/-}$ blastocysts. (B) RT-PCR analysis shows PIMT mRNA expression in E3.5 day wild-type ($PIMT^{+/+}$) blastocysts but not in E3.5 $PIMT^{-/-}$ blastocysts. (C) PIMT is expressed in all cells of E3.5 day wild-type $PIMT^{+/+}$ blastocysts but not in mutant $PIMT^{-/-}$ blastocysts. Immunostaining for Nanog and Oct4 reveal expression of these transcription factors in ICM in wild-type $PIMT^{+/+}$ (16/16 embryos) but not apparent in ICM of $PIMT^{-/-}$ blastocysts (5/5 embryos). Immunostaining for trophectoderm marker Cdx2 reveals that Cdx2 is expressed at subdued level in $PIMT^{-/-}$ blastocysts (8/9 embryos). Dapi staining reveals fragmentation and reduction in the number of nuclei in $PIMT^{-/-}$ blastocysts (17/19 embryos).

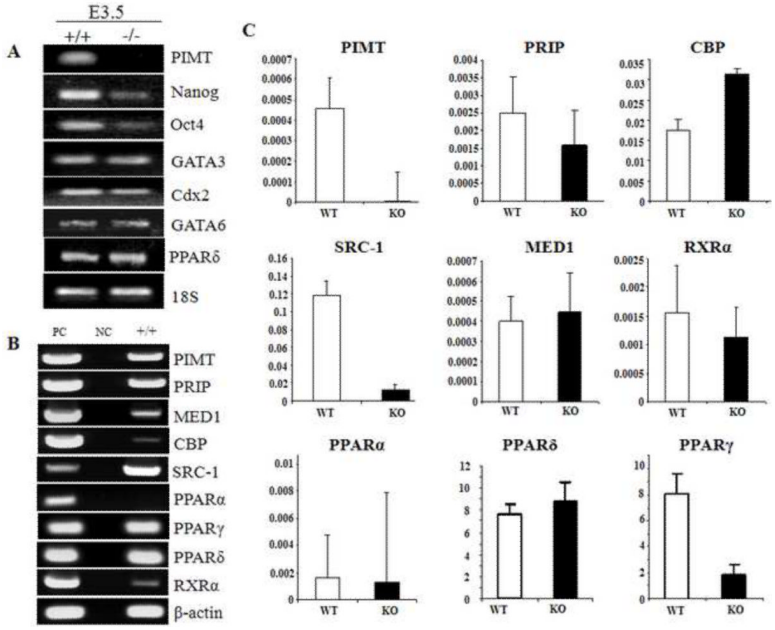

Fig. 6.

Expression of selected blastocyst markers, coactivators and nuclear receptors in E3.5 day blastocyst. (A) RT-PCR products from 6 pooled PIMT$^{+/+}$ and 6 pooled PIMT$^{-/-}$ E3.5 day blastocysts show reduction in ICM markers in PIMT$^{-/-}$ blastocytes. (B) RT-PCR products derived from 6 pooled E3.5 wild-type (PIMT$^{+/+}$) blastocysts reveal prominent expression of transcription cofactors PIMT, PRIP, SRC-1, and MED1 and nuclear receptors PPARδ and PPARγ. CBP and PPARα expression is not evident. PC, positive control, adult mouse liver RNA; NC, negative control, without reverse transcriptase. (C) Relative levels of expression of PIMT and other molecules in PIMT$^{+/+}$ and PIMT$^{-/-}$ E3.5 blastocysts. Total RNA isolated from pooled PIMT$^{+/+}$ and PIMT$^{-/-}$ E3.5 blastocysts (6 each group) was reverse transcribed for real time-PCR analysis. The specific amplification of target gene was normalized with 18 S RNA signal and arbitrary values are shown.

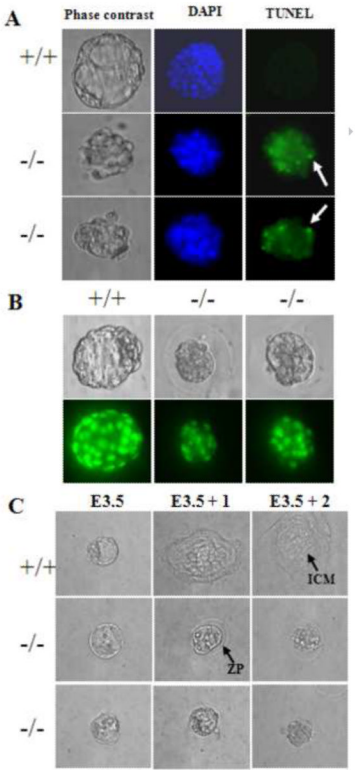

Fig. 7.

Evaluation of blastocysts for apoptosis, cell density and outgrowths. Representative examples of blastocysts isolated from PIMT$^{+/-}$ intercrosses at E3.5. (A) E3.5 blastocysts were cultured for 48 h and apoptotic cells identified using a fluorescent TUNEL assay (green fluorescence). Changes were assessed by phase contrast microscopy, DAPI staining and nuclear localization of TUNEL positivity. Excessive apoptosis is noted in 10/15 PIMT$^{-/-}$ blastocysts (*arrows*) and 2/25 PIMT$^{+/+}$ blastocysts. Membrane blebbing is prominent in phase contrast images of PIMT$^{-/-}$ embryos. (B) E3.5 blastocysts were cultured for 2 days at 37°C in ES cell medium that contained SYTO16 to vitally stain DNA. After live observations by phase contrast microscopy (upper panels), and fluorescence microscopy (lower panels), embryos were genotyped. PIMT$^{-/-}$ blastocysts showed reduction in cell number in comparison to PIMT$^{+/+}$ embryos. (C) Blastocysts in culture. All embryos were photographed every 24 h using phase contrast microscopy and genotyped at the end of culturing. Representative PIMT$^{+/+}$ (+/+), and PIMT$^{-/-}$ (−/−) blastocysts cultured in vitro for 2 days: E3.5 (day 0), E3.5 + 1 (day 1), and E3.5 + 2 (day 2). PIMT$^{-/-}$ embryos showed defects in hatching from zona pellucida and some hatched blastocysts were loosely anchored and failed to show robust proliferation. PIMT$^{+/+}$ embryos were composed of outgrowths of ICM. Some PIMT null embryos remained unhatched with intact zona pallucida (ZP).

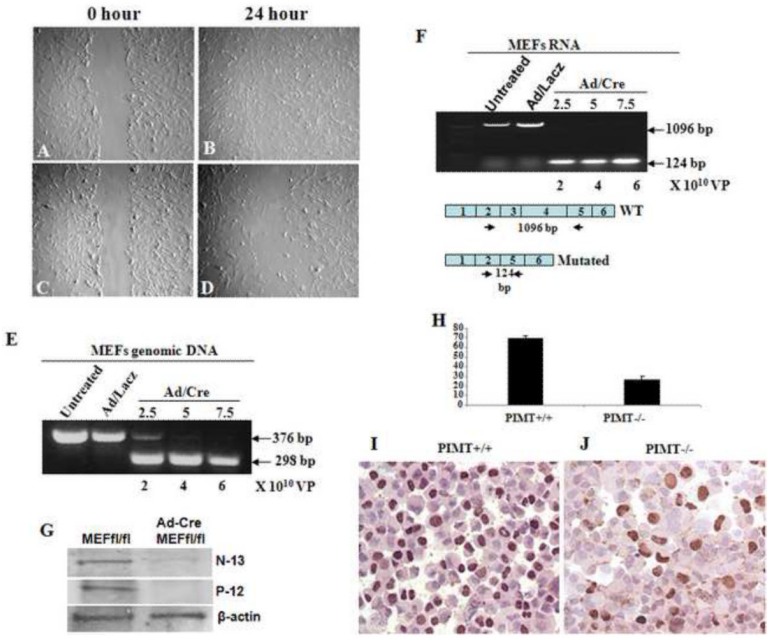

Fig. 8.

Defective motility (wound healing) of PIMT$^{-/-}$ MEFs. MEFs derived from PIMT$^{flox/flox}$ embryos were cultured to form a near confluent monolayer and migration monitored for 24 h in a scratch wound assay in uninfected (A, B), and adeno-Cre infected (C,D) conditions. This assay was repeated 5 times. (E) PCR based genotyping for PIMT gene deletion in MEFs. PIMT$^{flox/flox}$ MEFs were infected with Ad/LacZ or Ad/Cre and genotyped after 24 h. MEFs infected with adeno-Cre virus (2.5, 5 and 7.5 μl) show disruption of PIMT gene. (F) RT-PCR analysis of Ad/Cre infected and uninfected MEFs by using primers designed from the exons 2 and 5. PIMT transcript is detected in untreated and Ad/LacZ infected MEFs showing 1096 bp band. In the Ad/Cre infected MEFs, 124 bp band was obtained which confirmed the deletion of exons 3 and 4. (G) Western blot analysis using two different PIMT antibodies show absence of PIMT protein with P-12 antibody and a faint band with N-13 antibody. Bromodeoxyuridine immunohistochemistry shows reduced nuclear labeling in PIMT null MEFs (H, J) as compared to PIMT+/+ MEFs (H and I).

TABLE 1

Genotypes of PIMT+/− intercross progeny: Embryonic lethality

Age (dpc)	No. of mice with indicated genotype			
	+/+	+/−	−/−	Total
Weanling	71	135	0	206
E 9.5	15	28	0	43
E8.5	8	17	0	25
E7.5	7	16	0	23
E3.5	20	40	15	75